PRELIMINARY DESIGN OF A SCALED ROTOR BLADE WITH VIBRATION AND NOISE CONTROL DEVICES

M. Ghorashi, T. Mikjaniec, B. Lynch, F.D. Ulker, M. Cha
A. Mander, D. P. Brassard, D. Feszty and F. Nitzsche

[1] Department of Mechanical and Aerospace Engineering
Carleton University
1125 Colonel By Drive, Ottawa, ON K1S 5B6, Canada
e-mail: dfeszty@mae.carleton.ca

Key words: Blade Vortex Interaction (BVI), smart rotor, active control, vibration, noise, smart spring.

Abstract: In this paper, the preliminary design and manufacture of the SHARCS (Smart Hybrid Active Rotor Control System) scaled rotor blade and its accompanying control systems are presented. The primary objective of this research is the simultaneous reduction of noise and vibration generated by a rotor blade. The simultaneous noise and vibration control is achieved using three active control systems. Wind tunnel tests will be implemented to evaluate the design and demonstrate that the combination of the control systems can reduce both vibrations and noise. The control systems are an Actively Controlled Flap (ACF), an Actively Controlled Tip (ACT) and an Active Impedance Control device (AIC also known as Smart Spring) that replaces the pitch link. The designed flap control system uses piezoelectric actuators and can deflect 4 degrees at a 3 per rev frequency. The anhedral tip is electric motor driven and deflects 20 degrees over a few seconds. Finally, the smart spring is to control the blade vibration by modifying its boundary conditions at the root. Using close Mach and Lock numbers as well as given natural frequencies of vibration, the SHARCS rotor was scaled in a manner so that aeroacoustic and aeroelastic similarities were maintained with a full-scale rotor blade. After a try on NACA 0012, the blade section NACA 0015 was chosen to accommodate the control systems. The symmetric geometry of this blade section and the symmetric lay-up of the composite laminates, help in preventing out of plane strains, and the coupling of bending and stretching in the composite blade that can result in warping due to the applied centrifugal load. The composite lay-up of the articulated blade was iterated and tested by finite elements method (FEM) so that the natural frequencies match the required ones closely. The final check point in blade design is stress and failure mode analysis that is currently under way.

1 INTRODUCTION

Helicopter rotor blades generate vibration and noise, which negatively affect the operation of a rotorcraft: vibration causes passenger discomfort and structural fatigue, limits the forward flight performance of a helicopter and increases maintenance costs and weight. Noise deteriorates the environmental impact of a rotorcraft and enhances acoustic fatigue. Vibration and noise reduction are therefore of primary importance to helicopter manufacturers and users and have thus received considerable research interest especially in the recent past years.

The main cause of noise and vibration generation in helicopters is the main rotor that is subjected to unsteady aerodynamics that characterizes high-speed forward, maneuvering and descent flight regimes. Low-frequency vibration is mostly generated by dynamic stall in the reverse-flow region at high forward speeds. High-frequency acoustic noise, however, is produced mainly in maneuvering and descent flight regimes when the rotor blades interact with the vortices shed by the tip of preceding blades, resulting in a phenomenon known as Blade Vortex Interaction (BVI). This interaction leads to an impulsive change in the blade loading that generates a pressure perturbation in the flow field above and below the rotor disk. This perturbation propagates as a sound wave below the rotor disk and reaches the ground in the form of a strong slapping noise.

The next generation of helicopters is expected to feature active control devices to suppress noise and vibration likely through Individual Blade Control (IBC), where each blade is individually controlled independently of its azimuth angle. Recent experiments with IBC in Europe indicated that both noise and vibration could only be reduced marginally at the same time, although significant reductions of each individually were reported in [1]. The explanation for this fact would be the apparent conflict of the philosophy used in the control objectives, i.e. “smoothing” the path of the blade for the objective of vibration reduction and, at the same time, avoiding intersection with the impinging vortices for the objective of noise attenuation.

The main aim of the SHARCS (Smart Hybrid Active Rotor Control System) project is therefore to develop a “hybrid” control concept consisting of separate flow control and structural control subsystems. This approach (idealized in Fig. 1) would have the potential to reduce noise and vibration simultaneously, in part because the problems of vibration and noise are handled by two completely independent feedback subsystems. According to Fig. 1, a SHARCS blade would feature three actively controlled subsystems: an Actively Controlled Flap (ACF) to alleviate vibrations, and Actively Controlled Tip (ACT) to reduce BVI noise and an Active Impedance Control (AIC) device placed at the blade root to attenuate the residual vibrations transferring to the rotor hub and tune the boundary condition of the blade at the root.

The ACF would perform flow control by alleviating the negative effects of dynamic stall on the retreating blades, thus reducing the vibration excitation loads at their origin, [2]. In this reference, not only the size of the flap was shown to be relatively small, causing little conflict with the structural integrity of the blade, but also relatively little actuator forces would be needed. The ACF also has the potential to alleviate vibrations due to other sources, such as BVI or the unbalanced loads due to rotor blade imperfections.

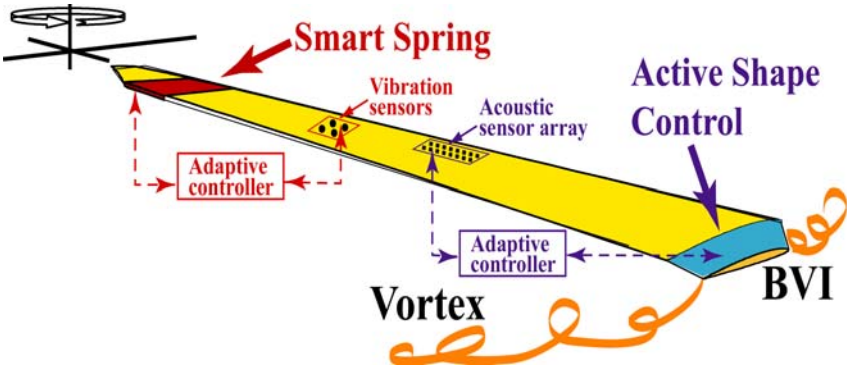

Figure 1: The SHARCS concept of hybrid vibration and noise control.

The ACT is used to alter the trajectory of the blade tip vortices and thus to vary their "miss distance" and the associated BVI noise. It has been demonstrated in separate studies that optimization of the blade anhedral tip angle can alleviate BVI at a fixed rotor attitude [3]. An adaptive mechanism taking advantage of this fact would be a flow control device specialized to perform noise control at flight conditions such as landing.

Finally, the Smart Spring is an active vibration controller that uses piezoelectric actuators to preferentially vary dry friction and stiffness of a structure. This device, if located at the blade root, could adaptively vary the dynamic stiffness of the blade and change its flexural characteristics. It is this effect that allows the control of the aeroelastic response of the entire blade. A real-time controller identifies the variations in the structural dynamics due to the unsteady aerodynamic environment and maximizes the vibration reduction performance. Simulations and laboratory tests have already verified the ability of the Smart Spring to adaptively vary the structural impedance properties in order to suppress low-frequency torsional aeroelastic vibrations of a fixed wing to buffet loads [4].

A major challenge in using the above subsystems is the actuator technology to be used. In the past, IBC was not fully developed due to the lack of actuators able to withstand the loads that characterize the helicopter rotor environment. Among the new solutions to achieve efficient IBC, the ones that involve smart structures are seen as most promising. One of the principal goals of the SHARCS project is therefore to demonstrate the ability of smart structures, employing multiple active material actuators, sensors and closed-loop controllers, to reduce both vibration and noise in rotorcraft applications. The overall goal of the SHARCS project is to develop, build and test a fully articulated four bladed aeroacoustically and aeroelastically scaled rotor model incorporating the above mentioned actively controlled subsystems.

SHARCS is an international project lead by the Carleton University from Canada, and involving University of Rome La Sapienza, University of Rome Tre and Politecnico di Milano from Italy and the National Technical University of Athens from Greece. The main industrial partners of the project are AGUSTA S.p.A. in Italy and SensorTech Ltd. in Canada (see [5] for more details). The present paper describes the second year progress of the project, namely the preliminary design of the scaled rotor blade and the associated subsystems.

2 SCALING FACTORS

The requirements for rotor scaling were set to ensure an acceptable platform to test the proposed vibration and noise reduction subsystems in a wind-tunnel test setup. For this, the

scaled rotor should share both aeroelastic and aeroacoustic similarities with the full-scale rotor.

Table 1. Design natural frequencies for aeroleastic similarity

Mode Shape	Natural frequency (per rev)
1st Elastic Flap	2.5 - 2.8
2nd Elastic Flap	4.2 - 4.7
1st Elastic Lead-Lag	4.5 - 5.5
1st Torsion	5.5 – 6

Aeroleastic similarity means that the structural response of the scaled blades, i.e. the natural frequencies in flapping, lead-lag and torsion, are similar to those of the full-scale blades. Table 1 shows the first four elastic modes and the corresponding natural frequencies of a BO105 rotor, which served as the basis for setting the aeroelastic similarity requirements.

Mach number similarity, on the other hand, means that the noise generated on the scaled rotor blades is within the range of that of the full-scale blades. Since helicopter acoustics is dominated primarily by BVI noise, which in turn depends on the tip Mach number, the second parameter to be maintained is the tip Mach number. The tip Mach number for the rotor to be designed was set to Mach 0.52.

An additional criterion for rotor scaling, concerns the Lock number, λ. It represents the ratio of aerodynamic excitation forces to inertial forces and is formulated as,

$$\lambda = \frac{3 \cdot \rho_{\infty} \cdot C_{L\alpha} \cdot c \cdot R}{m} \tag{1}$$

where, ρ_{∞} , $C_{L\alpha}$, c, R and m stand, respectively, for the air density, the lift curve slope, the blade chord, the rotor radius (includes the blade length and any offset value from the rotor axis) and the mass of the rotor blade including the actuators and corresponding mechanisms.

Lock number similarity would ensure that the excitation forces imposed on the model blade correspond in scale to those of the full-scale rotor. Typical Lock numbers of full-scale rotors are around 5 to 6. However, with the added weight of the actuators, it is usually difficult to maintain the requirement of Lock number similarity (in [6], a Mach scaled rotor blade with active tips lead to a Lock number of only 2.55).

3 BLADE GEOMETRY

The model rotor was scaled in such a way that it can be tested in a wind tunnel with 4m x 4m test section. To avoid wall effects, the rotor radius was set to 1.096 m. This defined, through the tip Mach number, the angular velocity of the rotor in hover is ω = 162.85 rad/s, i.e. N = 1555 rpm. Similar to the BO105 rotor, the scaled articulated rotor has 4 blades. Its chord length is 80 mm, resulting in a rotor solidity of 0.093. The tip of the blade is defined through a leading edge sweep angle of 12° from 0.9R outboard and a tip chord length of 40 mm. The root cut-out is 126 mm. Furthermore, the blade is twisted according to the twist law shown in Fig.2.

After a try on NACA 0012, the NACA 0015 airfoil was finally selected for the blade airfoil. At the given tip Mach number, this airfoil appeared to have the largest possible thickness,

minimizing transonic effects, yet maximizing space for the actuators and the corresponding mechanisms. The chosen symmetric airfoil and the symmetric blade composite lay-up (discussed in section 4) are beneficial in reducing warping of the blade skin due to centrifugal loads. At the tip, the blade gradually changes shape to a NACA 0008 airfoil.

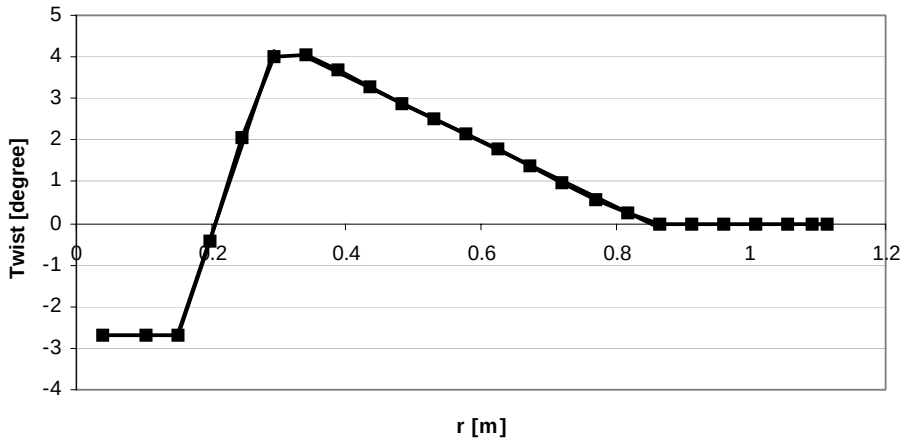

Figure 2. Twist distribution for the SHARCS blade.

The actively controlled subsystems are incorporated in the following manner. The actively controlled flap (ACF) spans from 0.65R to 0.85R and its chord length is 15% that of the blade. The required flap deflection is at least 4° down at a 3 per rev frequency. The flap size and actuation were selected based on earlier studies in [2] and are viewed as the best compromises between structural integrity, manufacturing and aerodynamic effectiveness. Note that the blade is mostly untwisted for the span where the flap is located. This was necessitated to enable the rotation of the flap (to keep the flap axis straight), and in this region the flap will be twisted to ensure a continuous aerodynamic twist.

The actively controlled tip (ACT) starts from 0.9R outboard, and it should be able to pivot at least 20° down. The ACT is viewed as a static controller, which will be kept at a constant deflection for a specific flight regime, so its full activation is allowed to last for several seconds (up to 10 to 30 s). The Smart Spring will replace the traditional pitch link and does not affect the blade geometry. The blade layout is illustrated in Fig. 3, with both the ACF and ACT locations highlighted.

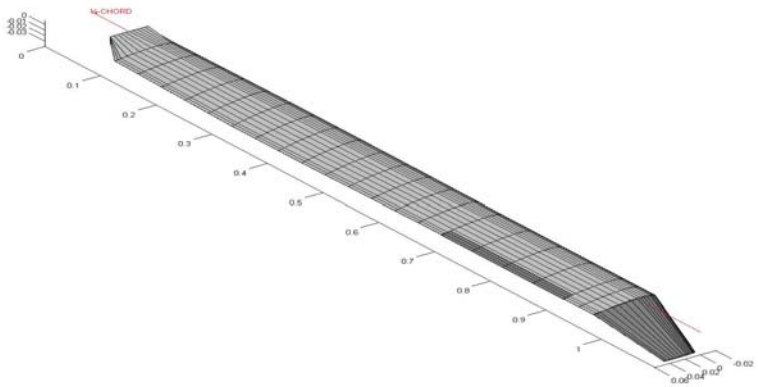

Figure 3. Layout of the SHARCS blade geometry.

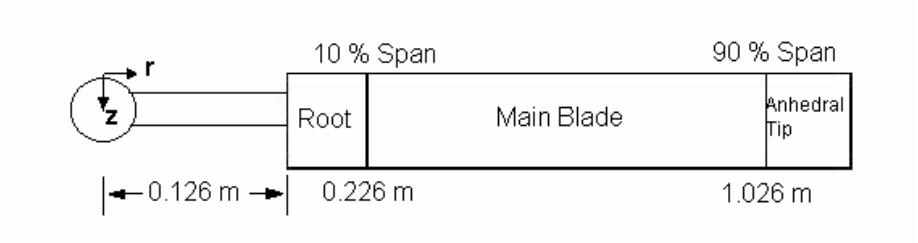

Figure 4. Schematic of SHARCS rotor blade

4 BLADE DESIGN

The SHARCS blade, sketched in Fig. 4, is to withstand the aerodynamic, actuator and inertial loads imposed on it during operation. At the same time, it is expected to have pre-assigned natural frequencies and mode shapes at the operating rotational speed.

Successful design of the blade requires a clear understanding of the aerodynamic and centrifugal forces that will act on it. However, these forces will not be known unless the blade geometry and its mass and stiffness distributions are known. Clearly, these details are not known beforehand. That is why the design of the blade is an inherently iterative process that starts with initial guesses. The outcome of the guesses (e.g. natural frequencies) is then compared against the requirements. This iteration leads to corrections on the guesses. Consecutive iterations are continued until convergence to an appropriate feasible (if not optimal) solution is obtained.

The solution algorithm of this design problem is illustrated in Fig. 5. This algorithm utilizes software packages on vibration analysis of rotating blades (Smart Rotor), finite elements method (ANSYS), composite materials elastic and failure properties (LamTech) and calculateion of load, stiffness and inertia properties of composites (developed at the German Aerospace Center (Deutsches Zentrum für Luft- und Raumfahrt [DLR]), [7]. The basic set of input values for the design of SHARCS blade are shown in Table 2.

Starting with initial guesses about mass and stiffness, the aerodynamic forces were calculated for a hovering case from Blade-Element-Momentum-Theory (BEMT) using Smart Rotor. This gave the spanwise distributions of lift and drag along the blade. However, the aerodynamic loads proved to be several orders of magnitude smaller than the centrifugal loads, therefore the design of the blade was largely dictated by the centrifugal forces.

Table 2. Input data for the rotor blade load program

Mass (m_x) [kg/m]	0.5355	Chord (c) [m]	0.08
Rotational Speed (Ω)[rad/s]	162.85	Angle of Attack (α) [°]	5
Hub Radius (r_0)[m]	0.126	No. of blades (z)	4
Outer Radius (R) [m]	1.096	F_{Maint} [N]	20
Air Density (ρ_∞) [kg/m³]	1.225		

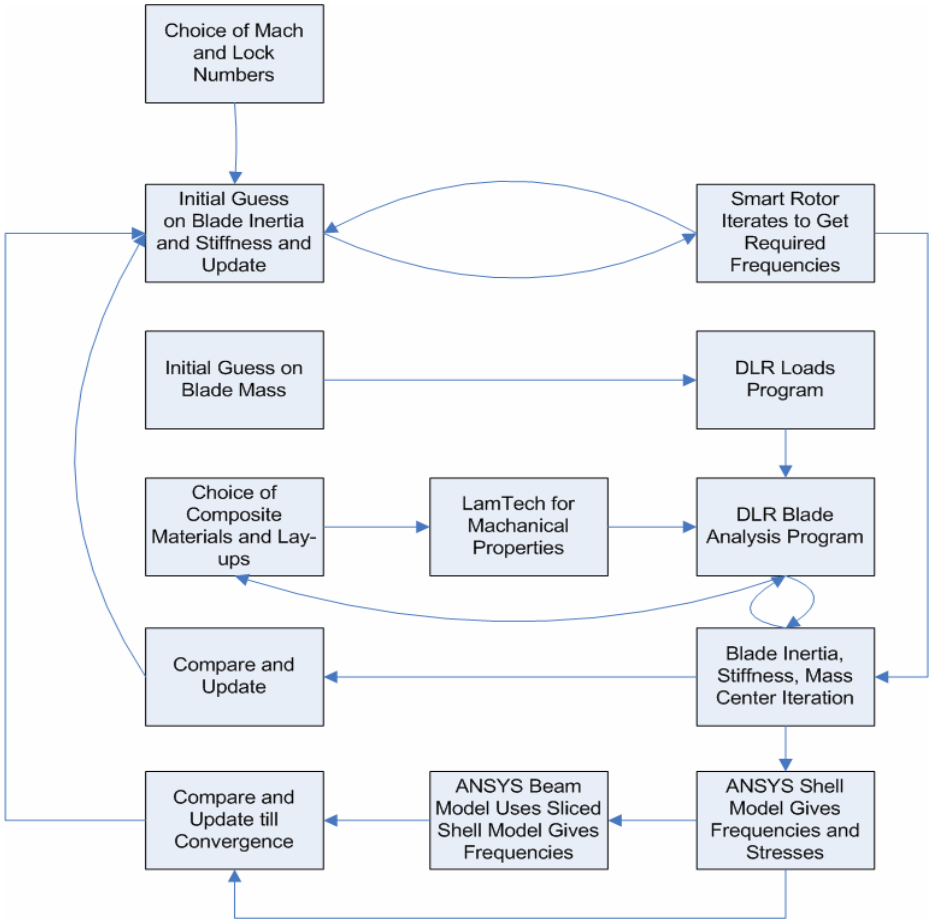

Figure 5. Flowchart of rotor blade design using Smart Rotor, ANSYS, LamTech and DLR-developed software packages.

Figure 6 illustrates the cross-section of the SHARCS rotor blade that utilizes the NACA0015 airfoil. It has a composite skin made of carbon fiber and glass fiber laminas with varying lay-ups along the chord. The lay-up at the trailing edge is [45/-45/0/-45/45], at the leading edge is [45/0/-45/0/-45/0/45] and between the two is [45/-45/-45/45]. Foam core and lead ballast are also implemented.

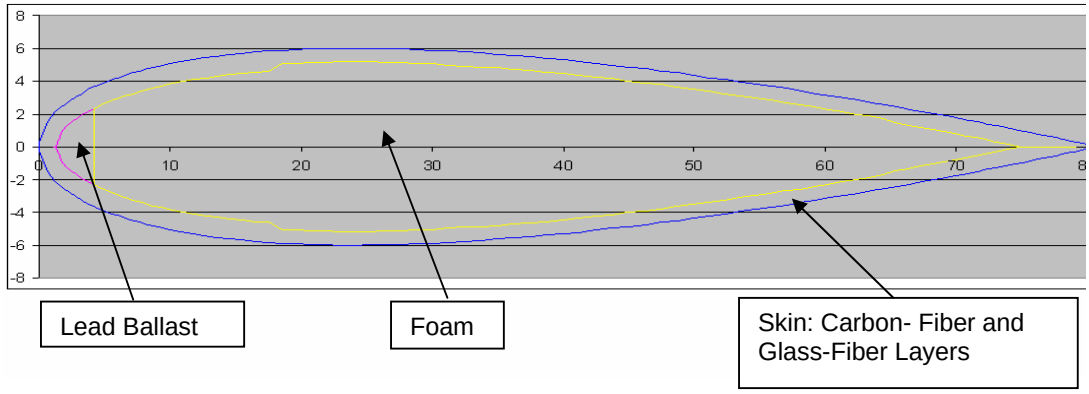

Figure 6. NACA 0015 Blade cross-section with composite layers, lead ballast and foam.

The angles are measured from the spanwise direction where the maximum loading, i.e. the centrifugal force is applied. The ±45° laminas are made of carbon fiber and the 0° ones are out of glass fiber. The laminates are all symmetric to ensure minimal out-of-plane strains as a result of the decoupling of bending and stretching in the laminates. The laminates are also balanced to achieve inplane orthotropic behavior. Ballast lead is included to shift the mass center of the section towards the aerodynamic center (about quarter chord). There are more fiberglass layers at the leading edge tip in order to simplify this mass center shift. Part of this ballast is also provided by the torque rod of the flap control mechanism discussed in section 6.

The FEM shell model of the rotor blade was prepared by ANSYS and is shown in Fig. 7.

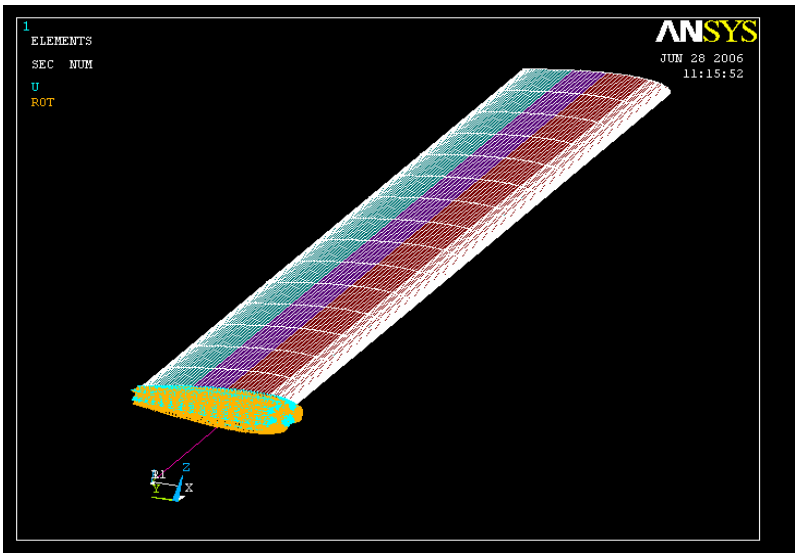

Figure 7. ANSYS shell model of the helicopter blade. Different colors represent different composite lay-ups along the chord.

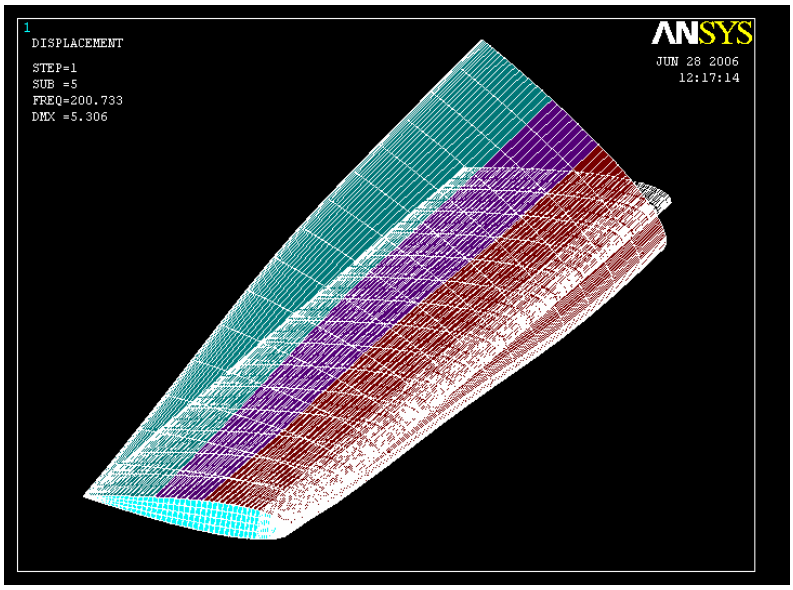

Figure 8. The first torsion mode of the blade compared to the undeformed blade.

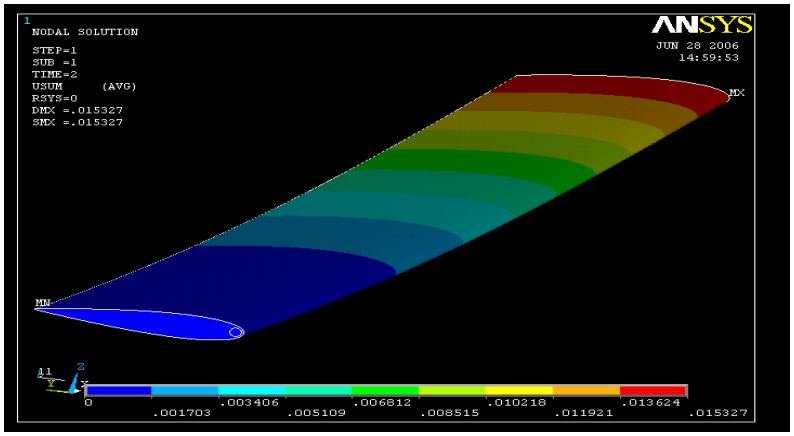

Figure 9. Displacement distribution along the rotating blade.

The model in Fig. 7 was used to obtain natural frequencies and mode shapes of the rotating blade using FEM. One of the acquired mode shapes is illustrated in Fig. 8. It also resulted in stress and displacement output as shown in Fig. 9. Figure 10 illustrates the output from ANSYS where the variation of the natural frequencies of the rotating blade against the angular velocity of the rotor (i.e. fan plot) for an alternative shell model that utilizes the NACA 0012 airfoil is presented. The fan plot preparation for the model based on the NACA 0015 airfoil is in progress.

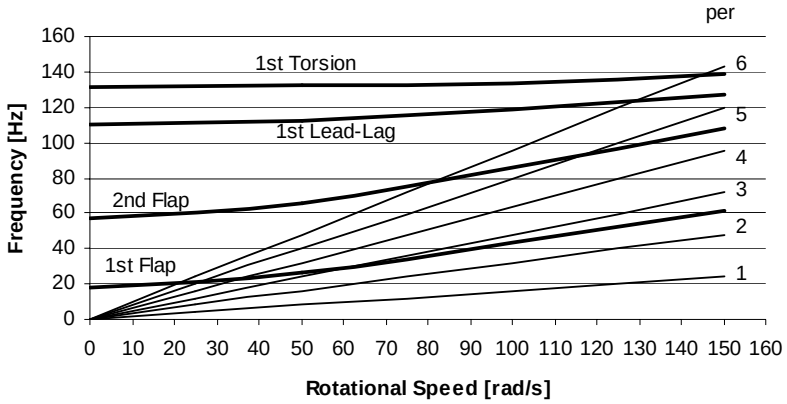

Figure 10. SHARCS rotor blade fanplot for NACA 0012 airfoil

Table 3 illustrates that the obtained natural frequencies of the NACA 0012 rotating blade satisfy the design requirements and are thus acceptable.

Table 3. SHARCS obtained rotating natural frequencies and the required frequency ranges

Mode Shape	SHARCS at 150 rad/s	Natural Frequency (per rev)
1st Elastic Flap	2.55	2.5 – 2.8
2nd Elastic Flap	4.53	4.2 – 4.7
1st Elastic Lead-Lag	5.33	4.5 – 5.5
1st Torsion	5.82	5.5 – 6

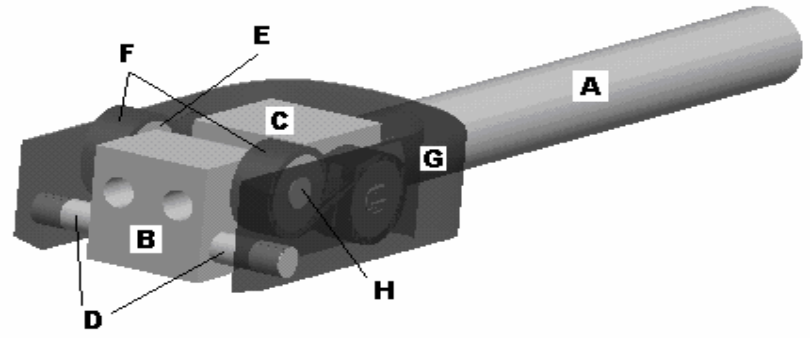

Figure 11: 3D rendering of the Actively Controlled Tip (ACT) actuator mechanism. A) screw, B) counter weight tip, C) counter weight holder, D) pin horseshoe, E) bearing, F) counter weight link, G) horseshoe, H) pin tip

5 ANHEDRAL CONTROL DESIGN

The Actively Controlled Tip (ACT) should enable the downward deflection of the blade tip up to 20°. The ACT is a static controller, i.e. the actuation can take place over several revolutions, lasting for about 10 to 30 s. For this reason, a screw type actuator design was selected. To decide on the size of the actuator, first the hinge moment created by the ACT had to be evaluated. It was found that the aerodynamic loading was negligible in comparison to the centrifugal force and the hinge moment was estimated to be as high as 3.39 N.m.

Figure 11 illustrates the anhedral control mechanism. The screw is rotated via an electric motor located at the blade root, through a light composite torque rod spanning through the blade. The torque rod can be placed close to the leading edge, thus providing useful ballast weight. Also, since it is hollow, it can be filled with ballast material to shift the mass center of the blade section toward the quarter chord. In this way, the mass of the torque rod will be used as a substitute for a portion of the lead ballast—reducing the mass of the whole blade assembly.

As the screw *A* rotates, the counter weight holder *C* is moved outward, which then pivots the anhedral tip (attached to *B*) downward. The counter weight holder is made of steel, so that its corresponding centrifugal force can help the actuation, thus reducing the power requirement of the actuator motor. Due to size limitations, the mechanism is very small (22 mm x16.7 mm x9 mm) with a mass of 35 g. The composite torque rod that actuates this system has a mass of about 40 g and the mass of the anhedral tab at the tip of the blade is 20 g. Based on the current selection of the screw thread and motor, the 20° deflection would be reached in a few seconds. Figure 12 shows the actuator as manufactured for the whirl tower tests.

Figure 12. The ACT mechanism as manufactured.

6 FLAP CONTROL DESIGN

The role of the Actively Controlled Flap (ACF) is to reduce vibrations due to unsteady aerodynamic effects—mostly dynamic stall on the retreating side of the rotor disc. The feasibility of the flap for such purpose has been demonstrated through 2D and 3D Computational Fluid Dynamics (CFD) simulations in [2]. It was found that the flap should be deflected with the frequency of about 3 per rev, to the deflections of about 10°. For the SHARCS experimental setup, the frequency requirement was maintained, but the maximum angular deflection was limited to only 4° due to the lack of powerful, and at the same time, compact enough actuators.

6.1 Flap Actuator Sizing

The flap actuator system should be able to overcome the hinge moments generated on the flap when deflected. The hinge moments were assessed by CFD simulations representing hovering conditions with the tip Mach number of 0.52. This is a conservative approach of evaluating the loads, since the flap will be actuated on the retreating side, where in forward flight the actual relative free stream velocity will be less. The maximum hinge moment, for angles of attack less than 10°, was found to be around 0.016 N.m.

The flap actuator system had to be designed small and light enough to fit inside the blade and does not produce significant centrifugal force, yet it had to be able to provide sufficient flap deflection and force to overcome the hinge moment. Following a preliminary study of hinge moment values, an APA 200M type piezoelectric actuator from Cedrat Ltd was selected to drive the flap actuation mechanism. The link lengths were then optimized to overcome the calculated hinge moments at the maximum angle of attack, and at the same time, maximize the flap deflection. In this optimization, the force deflection curve of the actuator (with a block force of 75 N and a maximum deflection of 240 μm) was used.

In the calculation of the link lengths of the flap mechanism in Fig. 13-a, the length L =15 mm was taken as a given constant (since it is already known how much free room the blade section has after installing the actuator mechanism). For the variable link lengths L_1 and L_2, the hinge moments were calculated using the force-displacement diagram of the actuator, assuming that the links are rigid. The selection of the link lengths was done considering the amount of deflection provided by the actuator and link system, and the hinge moments that have already been calculated from the CFD results for the maximum angle of attack of 10°.

Figure 13-b provides the variation of the hinge moment in terms of the flap deflection angle β (positive downwards) for a constant length L_1=16 mm, and a variable length L_2. Finally, considering the hinge moment values and design requirements, L_2 =2 mm was chosen.

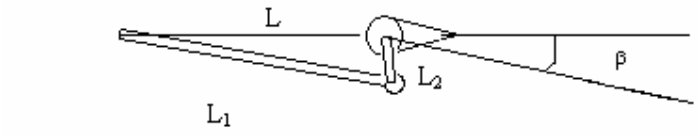

Figure 13-a. The flap actuation mechanism.

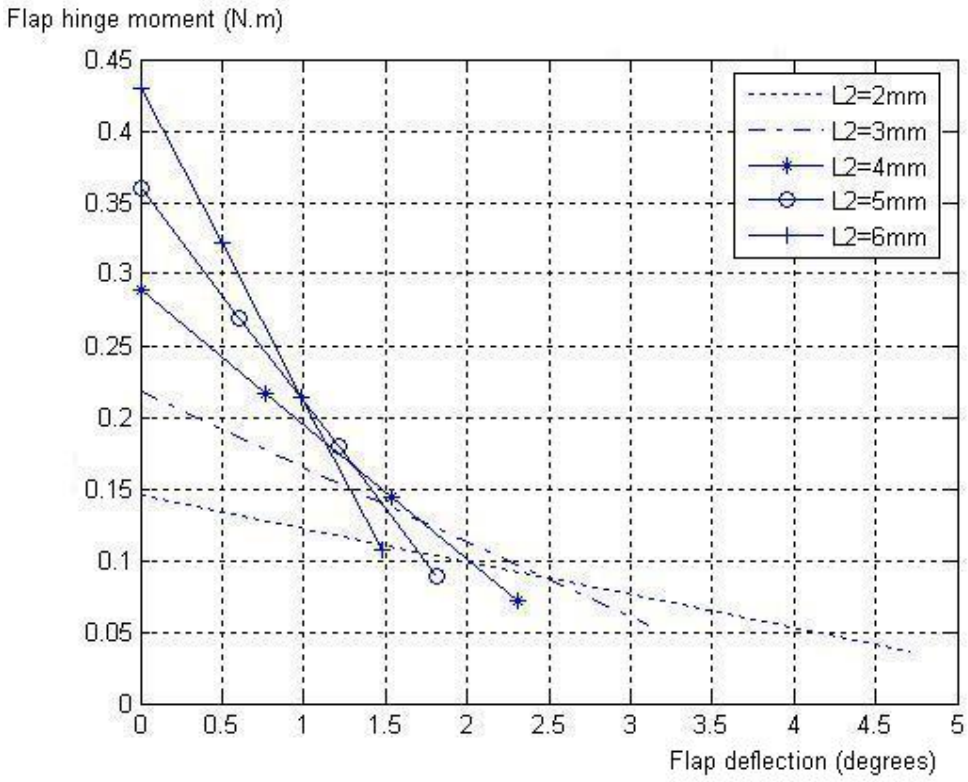

Figure 13-b. Presentation of the flap link length optimization results. (Flap hinge moment versus flap deflection for various values of L_2 and a 10˚angle of attack).

6.2 ACF System Analysis and Design

The parts of the actuator assembly of the trailing edge flap needed to be sized properly in order to fit within the interior of the SHARCS blade, while accomplishing the kinematic response required by the design of the controller.

Kinematically, the system is a slider-crank mechanism where the linear input displacement given by the piezoelectric actuators is converted to an angular displacement. Kinetically, the actuator force is used to support the hinge moment at the output. At the same time, the system must be supported against the centrifugal loads of its own mass. To this end, the linkage includes a surface, which would mate with a single roller, and provides a normal force counterbalancing (at least partially) the centrifugal loads. However, reaction forces due to the actuators as well as unbalanced centrifugal forces are eventually imposed on the blade and thus, their details should be considered in the final design of the blade (section 4).

Another design consideration is the stiffness of the parts within the system. For the purposes of accurate and predictable control, it was required that each part of the linkage has minimal deflection (i.e. enough stiffness) under the expected loads. However, increase of the stiffness should be made without corresponding increase in inertia and centrifugal loads. Therefore, some optimization was done to ensure that both the mass of the system and the stiffness values of the links remain acceptable.

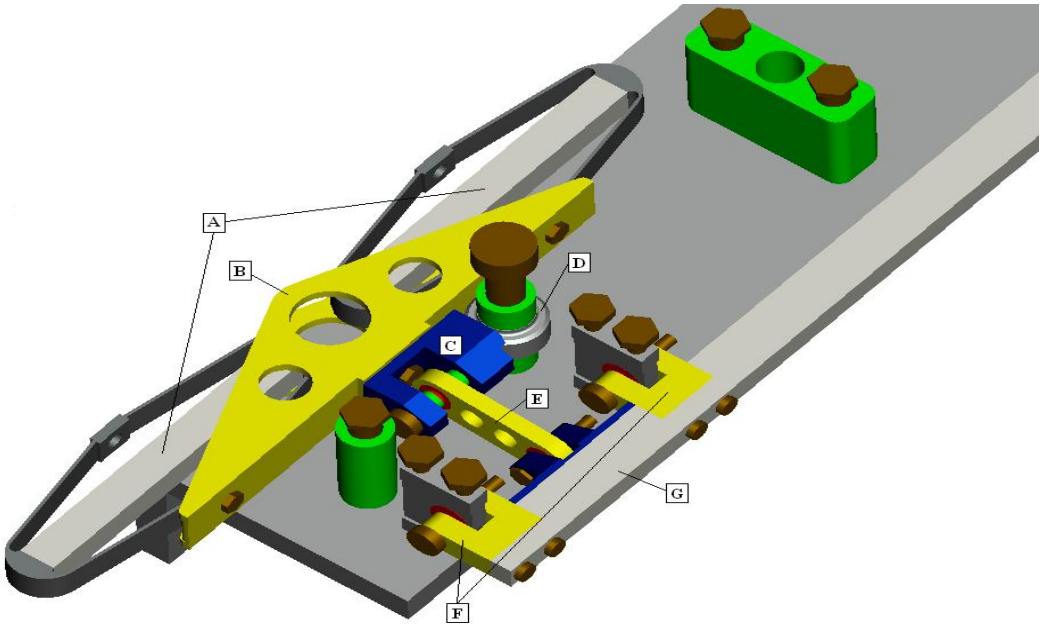

Figure 14. 3D rendering of the Actively Controlled Flap (ACF) actuator design, as prepared for the whirl tower tests. A) peizoelectric actuators, B) actuator pairing block, C) slider transmission block, D) roller sub-assembly, E) control rod, F) flap hinges, G) flap.

The design of the system was also heavily affected by the scale of the blade. Many difficulties encountered in the design of the assembly were mainly due to a lack of miniature bearings and fasteners. For instance, ball joint bearings (which would alleviate bending reactions within the linkage) could not be used due to the width and height of the housings. Furthermore, some linkage arm lengths were smaller than the diameter of the connecting pins, requiring a more creative design of the connection. In order to minimize mass, almost all of the parts were chosen to be machined out of an aluminum alloy. However, fasteners, bearings, and the roller are expected to be steel. Figure 14 illustrates the flap assembly as prepared for the whirl tower tests.

The system was finally designed to accommodate multiple actuator configurations: a single actuator, two actuators in series, and two actuators in parallel. The final configuration required that an extra part be designed to transmit the forces from two parallel actuators into one connection. The total mass of the flap actuation mechanism is 42 g.

7 SMART SPRING

The structural control in SHARCS is performed by an Axial Impedance Control (AIC) system substituting the conventional pitch link. This system is being entirely designed at Carleton University. The basic idea behind AIC is to adaptively alter the stiffness, damping and effective mass of the blade to control its structural response. The changes happen at the root of the blade and in this way, by changing its boundary condition; the response of the blade can be tuned. In this design, the actuators are not used against the applied loads, but they change the response indirectly by adjusting the boundary conditions. One example of such mechanism is shown in the conceptual drawing in Fig.15, optimized to exploit the large stiffness and bandwidth of piezoelectric materials to perform an indirect-active vibration of axial loads.

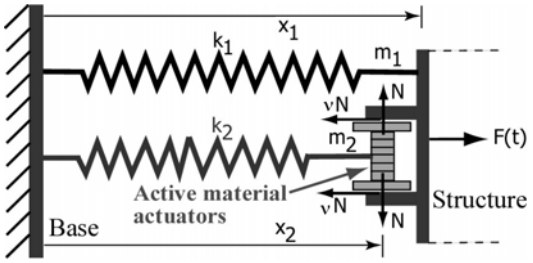

Figure 15. The Smart Spring concept illustrated.

The primary advantage of such a system, compared to other piezoelectric actuator based approaches, is that the device does not rely on the piezoelectric actuators to achieve high stroke and force simultaneously (which requires high power and high voltages). Rather, the device only requires the actuators to produce micro displacements to generate relatively high actuation forces. As such, the stacked piezoelectric actuators are able to achieve sufficient forces with less than 100 V peak-to-peak. In fact, since the actuators do not directly act against applied loads, they do not need to consume much power; the power is consumed only to change the impedance at the boundary condition.

The prototype system, which utilizes the concept shown in Fig. 15 is presently under development. Figure 16 illustrates a full scale test bench that allows the testing of the AIC subsystem and has been set up at Carleton University. It incorporates a full-scale blade linked to shakers and a test model of the AIC device. The test model utilizes piezoelectric actuators SJ12-50-1010-00 from SensorTech Ltd., Canada and magneto-rheological controllable fluid damper RD-1097-01 from Lord Corporation, USA that are used to adaptively tune the damping of the system.

In collaboration with University of Rome “La Sapienza”, the experimental system identification of the impedance control device was completed in 2005 [5]. This was the first step of the general task of developing the structural control subsystem (software and hardware). The design of the small-scale, more compact version of the AIC is currently underway.

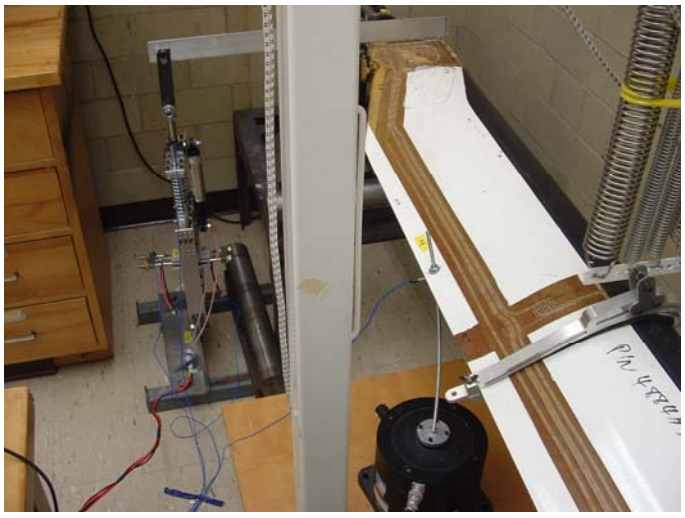

Figure 16. The Active Impedance Control device (AIC) test bench.

8 CONCLUSIONS

Preliminary design of the SHARCS scaled rotor blade was presented. The rotor incorporates three independent actively controlled subsystems for simultaneous reduction of noise and vibration. The preliminary design of the composite blade structure showed that due to the added weight of the actuators, corresponding mechanisms and necessary reinforcement of the blade (due to the increased loadings and the necessary ballast weight) the Lock number could not be kept on the levels of conventional helicopter blades. However, the targeted Lock number of 3.6 is still higher than what other researchers have reported for similar systems, demonstrating the effectiveness of the design. The aeroelastic and aeroacoustic similarity of the blade was satisfactorily ensured. The design of the actively controlled subsystems was dominated mainly by the given space limitations and the excessive centrifugal loads. The Actively Controlled Flap (ACF) is actuated via a piezoelectric stack actuator and should be capable of producing 4° deflection at 3 per rev actuation frequency. The Actively Controlled Tip (ACT) should be capable of producing 20° downward deflection within a few seconds. The design of the small-scale Active Impedance Control (AIC) device is underway. An iterative algorithm for the efficient design of the composite blade was prepared and used. It utilizes various design and analysis tools and implements FEM to choose the appropriate composite lay-up that maximizes the strength to weight ratio of the structure and at the same time provides the required natural frequencies and mass center location. Work on the remaining tasks of the SHARCS rotor design is in progress and wind tunnel tests are to take place in the fall of 2007.

9 ACKNOWLEDGEMENTS

This project was funded by the Natural Sciences and Engineering Research Council of Canada (NSERC) and Manufacturing and Materials Ontario (MMO). The authors would also like to thank AGUSTA S.p.A. and DLR Braunschweig for providing support and expertise in developing the model rotor.

10 REFERENCES

[1]. W. R. Splettstoesser, et. al., “The HELINOISE aeroacoustic rotor test in the DNW – test documentation and representative results”, DLR-Mitt. 93-09, DLR, Braunschweig, Germany, 1993.
[2]. G.L. Davis, D. Feszty and F. Nitzsche., “Trailing edge flap flow control for the mitigation of dynamic stall effects”, paper No. 053, 31st European Rotorcraft Forum, Florence, Italy, 12-14 September 2005.
[3]. T. Aoyama et al., “Calculation of rotor blade-vortex interaction noise using parallel Super Computer,” Paper 81, Proceedings: 22nd European Rotorcraft Forum, The Royal Aeronautical Society, Vol. 2, 1996.
[4]. F. Nitzsche, D. Zimcik, V. Wickramasinghe and C. Yong, “Control laws for an active tunable vibration absorber designed for aeroelastic damping augmentation,” The Aeronautical Journal, Vol. 108, No. 1079, 2004, pp. 35-42.
[5]. F. Nitzsche, et al., “The SHARCS Project: Smart Hybrid Active Rotor Control System for noise and vibration attenuation of helicopter rotor blades,” paper No. 052, 31st European Rotorcraft Forum, Florence, Italy, 12-14 September 2005.
[6]. A. Bernhard and I. Chopra I., “Hover test of a Mach-scaled rotor model with active blade tips,” Journal of the American Helicopter Society, Vol. 47, 2002, pp. 273-284.
[7]. Möller, C., “Strukturelle Auslegung eines Modellrotorblattes mit aktiver Verwindung,” Deutschen Zentrums für Luft- und Raumfahrt, Germany, Tech. Rep. Matrikel Nr. 2501172, 2004.